Diagnostic imaging techniques of the respiratory tract of sheep

Castells, E.[1]; Lacasta, D.[2]; Climent, M.[3]; Pérez, M.[1]; Sanromán, F.[1]; Jimenez, C.[2]; Ferrer, L.M.[2]

[1]*Centro Clínico Veterinario de Zaragoza. Spain.*

[2] *Animal Pathology Department. Veterinary Faculty of Zaragoza. Spain.*

[3] *Anatomy, embryology and animal genetics Department. Veterinary Faculty of Zaragoza. Spain.*

Corresponding autor: lmferrer@unizar.es

ABSTRACT

Diagnostic imaging techniques are very useful non-invasive methods to obtain medical images for the diagnosis of respiratory diseases in sheep.

The use of ultrasound and thermographic cameras must be enhanced at farm level with the objective of assisting in the diagnosis of major respiratory diseases present in sheep farms. X-ray and, particularly, computed tomography are very interesting tools to facilitate the understanding of the main pathological processes in sheep, especially at the respiratory level.

This article shows more than 40 images of thermograms, X-ray, ultrasonography and computed tomography of the most significant respiratory diseases in sheep.

Keywords: sheep, respiratory tract, diagnostic imaging techniques, thermography, ultrasonography, X-ray and computed tomography

1. Introduction

Diagnostic imaging techniques are non-invasive methods to obtain medical images for the diagnosis of diseases. Diagnostic imaging also establishes a database of normal anatomy and physiology as a reference to identify abnormalities in the different species.

For the diagnosis of respiratory diseases, the most useful diagnostic imaging techniques are ultrasonography, radiography, infrared thermography and computed tomography. Although it is obvious that some of these techniques will not be applicable in field conditions, these have been introduced in this article for scientific purposes and to provide a better understanding and comprehension of some respiratory pathologies.

Ultrasonographic examination has been widely used in the diagnosis of pregnancy in sheep; however it does not play still a major role in general clinical practice for the diagnosis of pathological disorders. Recently, Scott et al. (2017) published a deep review on the use of ultrasonography for the diagnosis of respiratory pathologies in sheep, thus not being this topic the main aim of the present article.

Infrared thermography is an innovative non-invasive tool that allows the remote measurement of the surface temperature of an animal. A thermal imaging camera captures and records the measurement and creates a colour thermal image, where each colour corresponds to a specified temperature (Redaelli and Caglio, 2013). These measurements can be evaluated to establish their physiological or pathological meaning, detecting inflammation of the superficial areas and becoming very useful to identify subclinical signs before the disease progresses (Luzi et al., 2013). These cameras will be very valuable in the diagnosis of upper respiratory tract pathologies in sheep.

X-ray imaging is based on the absorption of X-rays as they pass through a patient's body. Depending on the amount absorbed in a particular tissue, a different amount of X-rays will pass through the body and interact with the detection device (X-ray film or other image receptor) to finally provide a 2-dimensional projection image of the tissues within the patient's body (radiography). Nowadays, this technique is the most commonly used for the diagnosis of respiratory diseases in small animals, yet in sheep production it has not a widespread use.

Finally, computed tomography, also known as CT scanner, is also based on the variable absorption of X-rays by different tissues. However, CT provides a different form of imaging known as cross-sectional imaging. The origin of the word "tomography" is from the Greek word "tomos" meaning "slice" or "section" and "graphe" meaning "drawing”. Therefore, this system provides images that are slices of the anatomy of the animal. For the moment, and due to the high price of these devices, CT is only used with research proposes in sheep, being very valuable to understand the different respiratory pathologies. In this article different CT images of the main respiratory pathologies in sheep are shown.

In order to improve the understanding of respiratory diseases and their diagnosis, the text has been divided into two parts: upper respiratory tract pathologies, those affecting nasal cavity and paranasal sinuses, nasopharynx and larynx, and lower respiratory tract pathologies affecting trachea, lung and pleura.

The devices used to perform the images shown in this article are:

Thermographic camera: FLIR E63900, T198547. Images were performed at the Ruminant Clinical Service of the Veterinary Faculty of Zaragoza, Spain.

Portable ultrasound machine: VET EICKCMEYER Magic 5000 3.5-5 MHz. Images were performed at the Ruminant Clinical Service of the Veterinary Faculty of Zaragoza, Spain.

X-ray equipment: Sedecal, portable generator. SP-vet-4.0 Model. Images were performed at the Equine surgery and medical service of the Veterinary Faculty of Zaragoza, Spain.

Computed axial tomography: General Electric Healthcare. Bivro model of two slides. Images were performed at the Centro Clínico Veterinario of Zaragoza, Spain.

2. Upper respiratory tract pathologies

2.1. Head

2.1.1. Enzootic nasal adenocarcinoma of sheep

Enzootic nasal adenocarcinoma (ENA) is a contagious chronic disease of the upper airways in sheep. It has been described in Spanish farms, but also in all over the world (except in New Zeeland and Australia). ENA prevalence in an affected flock is variable, ranging from 0.1-15% and usually several cases are observed in the same flock. ENA is caused by an oncogenic retrovirus, ENTV-1 (Enzootic nasal tumour virus), that induces neoplastic (adenocarcinoma) growth of the secretory cells from the ethmoidal mucosa (De las Heras et al., 2018). First, a continuous unilateral serous discharge appears to evolve to a bilateral one, causing loss of hair around the nose. The disease is also known as “washed nose disease” (Ferrer et al., 2002). As the tumour grows, the bone around it undergoes pressure and become deformed, being even possible to deform the whole skull in severe cases, provoking exophthalmos and skin fistulation. Furthermore, ENA induces inspiratory dyspnea and snoring sounds. At necropsy, tumour is soft, grey or reddish-white in colour with a fine granular surface and it is covered with clear mucus.

For the diagnosis of this disease, **Infrared thermography** will be a useful tool. Thermographic camera performs pictures which present a colour scale that covers from cold (green and blue) to hot (yellow, orange, red and white). In the thermal picture (thermogram) of the nostril of a healthy animal, blue and green colours are found (Figs. 1a-1b). This is due to the fact that the air is passing through the nostril refrigerating the area. However, in ENA cases, the thermography shows reddish or even white colours in the posterior segment of the nose, matching the hottest areas (white colour) with the ethmoidal bone, where the ENA is located (Figs. 1c-1d). The nasal cavity presents also a red colour because, due to the obstruction provoked by the tumour, air cannot pass through the nose cooling the area.

In **radiography**, loss and deformation of the bone tissue in the ethmoidal area can be observed. A grey mass occupies the inside of the nasal chamber, pushing up the nasal bone in a more advanced stage of the disease (Fig. 2a).

Ultrasonography is not a very useful technique for the diagnosis of ENA. Only in the case that the nasal bone is destroyed and becomes a soft tissue, it is possible to see an echogenic tissue in the ethmoidal area with the transducer (Fig. 2b).

The last method described is the **computed tomography (CT)**. This device takes pictures around the whole skull and makes sections or slides of it, being the best method to visualize tissues comparing to other methods. Therefore, in ENA cases, this method shows the destruction of the ethmoidal bone, the lithic curse of the nasal bone and the soft tissues growing, even before the nasal bone is destroyed and the face deformed (Figs. 2c-2d).

2.1.2. Chronic proliferative rhinitis

Chronic proliferative rhinitis (CPR) in sheep has been associated with *Salmonella enterica* subsp. *diarizonae* serotype 61:k:1,5 (7) and causes an inflammation of the ventral nasal turbinates that produces uni-or bilateral thick seromucous nasal discharge, together with wheezing and snoring. These signs persist for several weeks or months, and worsen with almost complete nasal obstruction caused by the presence of proliferating tissue, often visible at the nares. Finally, animals develop severe respiratory distress with a striking mouth breathing (Lacasta et al., 2012). Pathological findings show a swollen ventral turbinates with a roughened surface. The section of the turbinate shows a proliferative tissue that is usually composed of multiple small white or yellow polypoid structures covered by mucus, although only a thickening of the mucosa can be observed (Lacasta et al., 2012; Rubira et al., 2018).

Thermographic images of CPR cases detect high temperatures (white colour) in the nostril area corresponding to the swollen ventral turbinate and a defect in nasal cavity ventilation (Fig. 3a).

In **radiography,** the affection of the ventral conchae can be seen with two lateral radiographic projections, one of each side. Although this disease does not affect the nasal bone as clearly as the enzootic tumour, an increased opacity is observed inside the ventral nose chamber (Fig. 3b).

Ultrasonography of CPR affected animals is not easy to interpret, mainly when the inflammation of the ventral conchae is not very severe. It is necessary to press the transducer against the nasoincisive notch until the swollen mass makes contact. More echogenic or hyperechoic tissue in the ventral area of the nostril is observed.

Finally, **computed tomography** enables to obtain a clear image of the damaged tissue and the different stages of development of the disease. It also shows the increase in size of swollen tissues and the bone destruction in more advanced cases (Figs. 3c-3d).

2.1.3.Oestrosis

Oestrosis is a common parasitism caused by a fly, *Oestrus ovis*, and their larval instars. This parasite is widespread in countries where there are a large amount of sheep and goats. Their presence is associated with hot and dry climates, such as Spain (Gracia et al., 2010), and also countries with extensive and semi-extensive production system flocks (Lucientes et al., 1998). The larvae produce a chronic inflammatory rhinitis, with serous, mucus, purulent or even haemorrhagic discharge from the noses. These secretions are linked to the stage of the larvae and also with the weather, because larvae stop their activity in some weather conditions (winter) and so do the secretions (Alcaide et al., 2003; Ferrer et al., 2002; Gracia et al., 2018). The prevalence of this illness is close to 85% in some Mediterranean countries.

For the diagnosis of this disease, thermal images and ultrasound are not used unless the parasitation is very severe. **Radiography** offers a poor capacity of detection, because the larvae body is not revealed. Only in some cases, the final stage of larvae (L3) can be seen (Fig. 4a).

Computed tomography offers better images. Tomographic pictures show the secretions, the swollen tissues of the turbinates and even the segments of the larvae (Figs. 4b-4c).

2.1.4. Intranasal Abscess

Finally, there are other causes of rhinitis, such as nasal abscesses. These processes are usually caused by bacterial infection and can be formed by pus or by caseous material (Ferrer et al., 2002; Benavides et al., 2015).

For the diagnosis of this pathology, **x-ray** shows a loss of the bone wall thickness and an increased soft tissue shape where the nasal bone disappears and turbinate bones loss their structure (Fig. 5a).

In **thermographic images** high temperatures (red and white colours) can be observed on the affected area (Fig. 5b).

Ultrasonography may only be used if the nasal upper side of the bone has suffered a lithic process. In this case, it is possible to put a transducer on the soft injured part and observe an echogenic capsule and underneath hypoechogenic tissues.

The **CT** allows a better view of all the mass and its location within the nasal cavity. Damaged areas and affected tissues can be differentiated as well as injured bone and the loss of its thickness in some places, or even abscess invasion from one to other nasal chamber (Figs. 5c-5d and 6a-6b).

2.2. Pharynx and larynx

Pharynx and larynx pathological disorders are not very common in sheep. Only chronic laryngitis associated with laryngeal chondritis has been commonly described in animals of the

Texel breed (Lane et al., 1987). Moreover, it was published a case received in our ruminant clinical service of Laryngeal hemiplegia in a Rasa Aragonesa Ram associated with *Sarcocystis* infection (Sáez et al., 2003). However, as in other species, processes such as abscesses, foreign bodies or tumours can be located in these areas. Ultrasound and tomographic assessments will allow evaluating the injury and getting a reliable diagnosis.

In the Fig. 7a ultrasonography of a ewe with a 7.27 cm abscess caused by *Corynebacterium pseudotuberculosis* is revealed. The big abscess pressed the larynx deforming it and causing respiratory distress. Figures 7b, 7c and 7d show an axial and sagittal CT view of the neck of this ewe with the CLA pyogranuloma on the epiglottis pressing the larynx.

2.3. Neck

2.3.1.Tracheal crushing

Tracheal crushing is a common disorder in our area of study. In a survey carried out by our research group, 100% of analysed farms had animals with lesion in some tracheal rings, 9.95% out of 7699 examined sheep were affected of tracheal damage. The presence of tracheal injury is clearly influenced by age; 63% of the affected animals were over 7 years (Ortega et al., 2017). Although the cause of this injury is not well defined yet, it seems to be a disorder associated with the management and the type of feeders during the periods of confinement of the animals.

In this pathology, **radiography** would be the gold standard diagnosis technique, because it allows assessing the lumen of the trachea and locating the injured area (Fig. 8a), while **computed tomography** would provide additional details about the process (Fig. 8b).

3. Lower respiratory tract pathologies

Ruminants are particularly sensitive animals to the development of lung pathologies, causing relevant economic losses. In lambs, apart from parasitic pneumonias, easy to diagnose with a coprological test, there is basically a pathology affecting the lower respiratory tract, ovine respiratory complex. However, in adults, there are several diseases that settle in the lower tract, making the diagnosis of respiratory diseases more complex (Lacasta et al., 2018). Based only in the clinical signs, these diseases are not easy to differentiate. Therefore, symptoms of the productive processes as gangrenous pneumonia, ovine respiratory complex or even pulmonary adenocarcinoma, can be very similar, becoming imaging diagnosis techniques a very useful tool to reach the final diagnosis.

In the study of lower respiratory tract pathologies, only ultrasonography, radiography and computed axial tomography will be shown, because thermography is not a valuable tool in these pathological processes.

3.1. Maedi-Visna disease

Maedi-Visna disease is an ovine disease caused by SRLV (small ruminant lentivirus), that induce a systemic infection that may affect in an immunomediated manner an array of target organs, such as lung, central nervous system, mammary gland and joints (Minguijón et al., 2015). The clinical syndrome is caused by interstitial pneumonia that produces severe dyspnea without productive sounds and progressive loss of bodyweight (Luján et al., 2018). However, when the illness is not so advanced, clinical signs can be confusing. Moreover, SRLV infects immunological cells promoting the development of other kind of lung injuries. In a survey carried out in our clinical service, 52.2% of the animals with interstitial pneumonia related to SRLV presented other lung injury as pleurisy, fibrinous pneumonia, abscesses or gangrenous pneumonia (Lacasta et al., 2016).

Radiography shows, in a more advance stage, a diffused interstitial pattern in all lungs (Fig. 9a).

The **ultrasound imaging** indicates a homogeneous echogenicity in all of pulmonary parenchyma (Fig. 9b), although is not easy to differentiate at the initial stages of the disease.

Computed Tomography provides a better detail of the lesion, highlighting the increased opacity in all the parenchyma associated with the interstitial pneumonia caused by MVV (Fig. 9c).

3.2. Ovine Respiratory Complex in adults

As ovine respiratory complex (ORC) in lambs, in adults, ORC is regarded as a complex disease, involving interaction among host (immunological and physiological), multiple etiological agents (bacteria and mycoplasma) and environmental factors (stressors) and it produces similar lesional pattern (Lacasta et al., 2018). A hyperacute or systemic form, characterized by hemorrhages, and acute and chronic forms, characterized by lung consolidation, can be present. Lung consolidation is shown as suppurative (catharral) or fibrinous pneumonia with different degrees of severity.

In a chronic pneumonia related to ORC, **radiography** shows an alveolar pattern, without an interstitial lesion (Fig. 10a). Opaque alveoli with fluid in bronchial lumen are seen. **Ultrasonography** displays areas of more echogenic tissue without a clear split of the normal tissue (Fig. 10b). In some cases, it is possible to find abundant purulent foci of different size and texture.

Computed Tomography reveals a better view of the injured areas. Collapsed lung areas are more opaque and whitish (Fig. 10c), while healthy tissue remains the typical grey colour of a lung full of air. It is interesting to highlight that air usually remains inside the thickest bronchia even when they are surrounded by pneumonic tissue. With the software associated to the CT scanner is possible to measure the affected area of the lung. Based on this measurement, the progression of the disease can be followed.

3.3. Ovine pulmonary adenocarcinoma

Ovine pulmonary adenocarcinoma (OPA) is a transmissible lung tumour of sheep caused by jaagsiekte sheep retrovirus (JSRV) which induces the transformation of secretory epithelial cells of the distal respiratory tract. Affected animals have dyspnea and moist respiratory sounds, caused by the accumulation of fluid in the respiratory airways. In the final stages of the disease, variable amounts of frothy serous pulmonary fluid (De Las Heras et al., 2003; Cousens et al., 2009) is discharged from the nostrils when the sheep head is lowered (“wheelbarrow” test). At necropsy, neoplastic lesions are diffuse or nodular, grey or purple in colour and have an increased consistency (Ortín et al., 2018).

In the **X-ray,** a nodular pattern can be observed at the beginning of the process with small and diffused nodules (Fig. 11a). Once tumour nodules converge and form larger lesions, they are more easily detected.

Ultrasonographic examination of ovine pulmonary adenocarcinoma involving the lung surface/visceral pleura reveals hypoechoic areas representing a tumour mass, defined dorsally by a broad hyperechoic line (Scott, 2017). Ultrasound displays echogenic areas that correspond with different-sized neoplastic nodules associated with OPA (Fig. 11b).

Computed tomography provides a clear picture of the tumour nodules inside the lung and their different sizes and locations. This technique also allows serial CTs to evaluate the progression of the disease. At first, it can be observed a nodular pattern with small and diffused dotted that converge in different-sized masses (Fig. 11c).

3.4. Verminous pneumonia

This pneumonia is caused by mechanical and irritant action of nematodes belonging to the order of *Strongylida*. The biggest one, *Dictyocaulus filaria*, affects caudal and diaphragmatic part of the lungs, and the small worms, belonging to the *Protostrongylidae* family (*Protostrongylus rufescens, Muellerius capillaris, Cystocaulus ocreatus* and *Neostronglylus linearis*), causes injuries in the dorsal and the diaphragmatic part of the lungs. These nematodes induce a response from the host that tries to surround and encapsulate the parasites, generating the typical nodules associated with verminous pneumonia.

X-ray images show alveolar and nodular interstitial patterns that forms a mixed pattern. Usually, lesions are located in the dorsal part of the lungs, opaquer on the damaged areas.

Ultrasonography reveals an echogenic zone surrounded by normal areas in the dorsal part of the lungs. If the areas of verminous pneumonia are small, they are not easy to see through this technique.

Computed Tomography, again, presents a better picture of nodular pneumonic areas located in the dorsal parts of the lung. Usually, small worms move on to the caudal-dorsal lung, making a line over the dorsal lung tissue with diffused borders (Figs. 12a-12b). An increased thickness of the caudal and diaphragmatic areas can be observed in the case of *Dictyocaulus filaria*.

3.5. Caseous Lymphadenitis

Caseous Lymphadenitis (CLA) is a disease caused by *Corynebacterium pseudotuberculosis* that results in the formation of pyogranulomatous lesions affecting mainly the lymph nodes (Fontaine and Baird, 2008). There are two clinical presentations: the external, also known as cutaneous or superficial, and the visceral form. While superficial form affects only lymph nodes, visceral presentation can affect both lymph nodes and the parenchyma of several organs, especially the lungs. Sometimes, these abscesses can compress other structures such as oesophagus or vagus nerve producing different syndromes (Fuzës et al., 2015).

When CLA affects a mediastinal lymph node, a **chest-x-ray** displays a radiopaque round mass usually localized forward of the heart, although sometimes, this mass appears behind it. Similar image is observed when the lesion is located in lung parenchyma, kidneys or mesenteric lymph nodes.

Ultrasonography is not the most useful diagnostic method for this pathology, because abscesses could be found deep inside the parenchyma and transducer cannot provide a clear picture of the CLA. Nevertheless, if abscesses are detected, a hyperechogenic round shape under the normal tissue is shown.

Computed tomography provides a specific image of the abscess, their location, and injured tissues involved in the disease. Frequently, there is an enhance area around the abscess and mineralization within abscess due to caseous necrosis (Figs. 13a-13b-13c).

3.6. Gangrenous pneumonia

Gangrenous pneumonia, also known as aspiration pneumonia or necrotizing pneumonia, is a pulmonary infection characterized by inflammation and necrosis due to inhalation of foreign substances. Foreign body drives environmental bacteria that produce foci of pulmonary necrosis with accumulation of a foul-smelling exudate that sometimes is also present in the main bronchus and trachea. In these cases, bad smell of exhaled air is a clear clinical sign of the disease (Lacasta et al., 2018).

An **X-ray** will show a mixed pattern (alveolar and interstitial) where the lesion is located. Affected areas show loss of opacity that sometimes can be mistaken for emphysema, although usually the lesion is surrounded by clear border.

Ultrasound images are clear, offering different echogenicity foci in all the affected area depending on the material inside the lesion (Fig. 14a).

Computed tomography shows the lesion with the adjacent tissues enhanced. Affected area shows necrotic tissue (dark or black) with diffused edges (Fig. 14b). Bronchia lumen cannot be seen due to the pneumonic damages, especially in the area where injury starts. As well, lacking-tissue caves can be observed in the most severe damaged areas (Fig. 14c).

4. Final remarks

Diagnostic imaging techniques are very useful tools for the proper diagnosis of respiratory diseases in sheep. The use of ultrasound and thermographic cameras must be enhanced at farm level, not only with reproductive purpose, but also with the objective of assisting in the diagnosis of major diseases present in sheep farms.

X-ray and, particularly, computed axial tomography are very interesting tools to facilitate the understanding of the main pathological processes in sheep, especially at the respiratory level, as it has been shown in this article. CT images allow analyzing slides of tissues of different thicknesses that offer very detailed images. These pictures may sometimes even improve the diagnostic results obtained at the *post mortem* study of the animals, because the structure of the tissues can be observed in greater detail. Furthermore, these techniques let us to observe the evolution of the lesions and how animals are recovering.

5. Acknowledgment

Authors would like to thank colleagues from the *Centro Clínico Veterinario of Zaragoza* for offering us the opportunity to obtain revealing CT images using their facilities and their CT scan. Furthermore, we would like to acknowledge Equine service veterinarians of the Veterinary Hospital at the University of Zaragoza for helping us with the x-ray interpretation.

Conflict of interest statement

The authors have nothing to disclose.

References

Alcaide, M., Reina, D., Sanchez, J., Frontera, E., Navarrete, I. (2003). Seasonal variations in the larval burden distribution of Oestrus ovis in sheep in the southwest of Spain. Veterinary Parasitology 118, 235-241.

Benavides, J., Gonzalez, L., Dagleish, M., Perez, V. (2015). Diagnostic pathology in microbial diseases of sheep or goats. Veterinary Microbiology 181, 15-26.

Cousens C., Thonur L., Imlach S., Crawford J., Sales J. et al. (2009) Jaagsiekte sheep retrovirus is present at high concentration in lung fluid produced by ovine pulmonary adenocarcinoma-affected sheep and can survive for several weeks at ambient temperatures. Research in Veterinary Science, 87, 154-156.

De las Heras, M., Ortin, A., Cousens, C., Minguijon, E., Sharp, J.M. (2003). Enzootic nasal adenocarcinoma of sheep and goats, In: Fan, H. (Ed.) Jaagsiekte Sheep Retrovirus and Lung Cancer. Current Topics in Microbiology and Immunology 275, 201-223.

De las Heras, M., Ortín, A., Borobia, M., Navarro, T. (2018). Enzootic Nasal Adenocarcinoma: an update. Small Ruminant Research (2018)

Ferrer, L.M., Garcia de Jalon, J.A., De las Heras, M. (2002). Athlas of ovine pathology. Servet Diseño y Comunicacion S.L. 184-187.

Fontaine, M.C., Baird, G.J. (2008). Caseous lymphadenitis. Small Ruminant Research 76, 42-48.

Füzes, K., Osorio, V., Lacasta, D. (2015). Timpanismo de rumen y abomaso en una oveja causado por una linfoadenitis caseosa. Número especial Septiembre 2015. Monográficos Albeitar.

Gracia, M. J., Lucientes, J., Peribanez, M. A., Castillo, J. A., Calvete, C., Ferrer, L. M. (2010). Epidemiology of Oestrus ovis infection of sheep in northeast Spain (mid-Ebro Valley). Tropical Animal Health and Production 42(5), 811–813.

Gracia, M.J., Ruíz de Arcaute, M., Ferrer, L.M.; Ramo, M., Jimenez, C., Figueras, L. Oestrosis: parasitism by Oestrus ovis (2018)

Lacasta, D., Ferrer, L.M., Ramos, J.J., Bueso, J.P., Borobia, M., de Arcaute, M.R., Figueras, L., Gonzalez, J.M., De las Heras, M. (2012). Chronic proliferative rhinitis associated with Salmonella enterica subspecies diarizonae in sheep in spain. Journal of Comparative Pathology 146, 72-72.

Lacasta, D.; González, J.M.; Navarro, T.; Valero, M.; Saura, F.; Ramos, J.J.; Ferrer, LM.; Ortín, A.; Jiménez, C. (2016). Respiratory diseases affecting adult sheep in Spain. Relationship between auscultation and lung lesion. Deutsche Veterinarmedizinische Gesellschaft and ECSRHM annual congress, Freiburg, Germany.

Lacasta, D., Fernández, A., González, J.M., Navarro, T.,Ferrer, L.M., Ramos, J.J. Other respiratory diseases affecting adult sheep. (2018)

Lane, J.G., Brown, P.J., Lancaster, M.L. and Todd, J.N. (1987) Laryngeal chondritis in Texel sheep. Veterinary Record, 121, 81-84.

Lucientes, J. Castillo, J.A., Ferrer, L.M., Peribáñez, M.A., Ferrer-Dufol, M., Gracia-Salinas, M.J. (1998). Efficacy of orally administered ivermectin against larval stages of Oestrus ovis in sheep. Vet. Parasitol. 75, 255-259.

Luján, L., Pérez, M., De Andrés, D., Reina, R. (2018). Lentivirus infection in small ruminants. (2018)

-Luzi, F., Mitchel, M., Costa, L.N., Redaelli, V. (2013). Thermography. Current status and advances in livestock animals and in veterinary medicine. Fondazione Iniziative Zooprofilattiche e Zootechniche Brescia.

Minguijón E., Reina R., Pérez M., Polledo L., Villoria M., Ramírez H., Leginagoikoa I., Badiola J.J., Garcíamarín J.F., De Andrés D., Luján L., Amorena B. & Juste R.A. (2015). Small ruminant lentivirus infections and diseases. Veterinary Microbiology, 181, 75–89.

Ortega, M., Gonzákez, J.M., Ramos, J.J., Ferrer, L.M., Ruiz de Arcaute, M., Lacasta, D., Gartziandia, A. and Espada M. (2017). Estudio de las alteraciones de la tráquea en el ganado ovino: descripción y prevalencia. XLII Congreso Nacional y XVIII Congreso Internacional de la Sociedad Española de Ovinotecnica y Caprinotecnia 2017, Salamanca, Spain.

Ortín, A., De las Heras, M., Borobia, M., Ramo, M., Ortega, M., Ruíz de Arcaute, M. (2018). Ovine pulmonary adenocarcinoma: a transmissible lung cancer of sheep, difficult to control

Redaelli, V. (2013) Thermography, current status and advances in livestock animals and in veterinary medicine (pp 41-46), Fondazione Iniziative Zooprofilattiche e Zootechniche, Brescia.

Rubira, I., Figueras, L. De las Heras, M., Bueso, J.P., Castells, E., Climent, M., Lacasta, D. (2018) Chronic proliferative rhinitis in sheep: Is its relevance increasing?

Sáez, T.; Ramos, J.J.; García del Jalón, J.A.; Unzueta, A.; Loste, A. (2003). Laryngeal hemiplegia in a ram associated with Sarcocystis species infection. Veterinary Record, (153) pp 27-28

Scott, P.R. (2017). Use of ultrasonographic examination in sheep health management – A general appraisal. Small Ruminant Research 152, 2-9.

Figure legends

Figure 1. 1a. Healthy animal. 1b. Thermogram of a healthy animal with normal refrigeration of the nostril (White circle). 1c. ENA affected animal (black arrow). 1d. Thermogram of an ENA affected animal. Reddish or white colours in the posterior segment of the nose matching with the

ethmoidal bone, where the ENA is located (black arrow). Red colour of the nostril due to obstruction and poor ventilation of the area (white circle).

Figure 2. 2a. Lateral radiographic projection of the head of a sheep with ENA (white arrow). 2b. Ultrasound image of the ethmoidal turbinate in a case of advance enzootic nasal adenocarcinoma in sheep. 2c. CT axial view of a ewe with enzootic nasal adenocarcinoma (bone filter), showing the affection of the nasal bone. 2d. CT 3D view of a sheep with enzootic nasal tumour (volume rendering). The lithic process in the nasal and lacrimal bones producing some holes in the bones is shown (white arrows).

Figure 3. 3a. Thermogram of a ewe with unilateral chronic proliferative rhinitis. White areas indicate swollen turbinate and the inability of a correct nasal cavity ventilation. 3b. Lateral radiographic projection of a ewe with chronic proliferative rhinitis affecting the ventral nasal turbinate. Swollen area is clearly seen in the image. 3c. CT axial image of a ewe with chronic proliferative rhinitis (bone filter). It can be observed the tissue invasion from the right to the left nasal chamber causing the nasal septum deformation (white arrow). 3d. CT 3D image of a ewe with chronic proliferative rhinitis (volume rendering).

Figure 4. 4a. Lateral radiographic projection of the head of a ewe parasitized by *Oestrus ovis* larvae. It is evident the difficulty to distinguish the larvae from the other tissues (white arrow). 4b. CT axial view of the head of a ewe parasitized by *Oestrus ovis* larvae (head filter). Larvae are shown in the picture (white arrow). 4c. CT sagittal view of the head of a ewe parasitized by *Oestrus ovis* larvae (bone filter). Larvae are indicated in the picture (white arrow).

Figure 5. 5a. Ventrodorsal radiographic projection of the head of a ewe with a nasal abscess caused by *Corynebacterium pseudotuberculosis*. 5b. Thermogram of a ewe with an abscess and rhinitis in the right side. 5c. CT of the head of a ewe with a nasal abscess (bone filter). Destruction of the nasal bone is cleared shown (white arrow). 5d. CT coronal view (soft tissue filter) of the abscess injuring the right nasal chamber and the right nasal bone of a ewe (white arrows). (Soft tissue filter).

Figure 6. 6a. CT sagittal view of a ewe's head with an abscess (soft tissue filter). 6b. CT 3D axial view of a ewe's head with an abscess (volume rendering). A hole (white arrow) in the nasal and maxillary bone caused by an abscess is shown (yellow circle).

Figure 7. 7a. CT sagittal view of a ewe's head with an abscess (soft tissue filter). 7b. CT 3D axial view of a ewe's head with an abscess (volume rendering). A hole (white arrow) in the nasal and maxillary bone caused by an abscess is shown (yellow circle). 7c. Ultrasonographic image of the neck of a ewe with a 7.27 cm abscess of caseous lymphadenitis pressing and deforming the laryngx. 7d. CT axial view of the neck of a ewe with a caseous lymphadenitis pyogranuloma pressing the larynx (soft tissue filter).

Figure 8. 8a. Lateral radiographic projection of the neck of a ewe with tracheal crushing. It is showed the stenosis in the medial fraction of the trachea. 8b. CT 3D sagittal view of the trachea of a sheep with the crushing of some tracheal rings.

Figure 9. 9a. Lateral radiographic projection of the thorax of a sheep with interstitial pattern. There is an increased opacity in the lungs due to infiltrate of lymphocytes in the interstitial tissue. 9b. Ultrasound imaging shows consolidated lung with high echogenicity in a clinical case of Maedi Visna disease. 9c. CT image of the thorax of a sheep with high opacity caused by interstitial pneumonia associated with Maedi Visna disease.

Figure 10. 10a. Radiography of the thorax of a sheep affected of ovine respiratory complex. It can be observed the alveolar pattern, expressed as white areas and diffused borders. 10b. Ultrasonographic imaging of a lung with fibrinous pneumonia associated with ovine respiratory complex. More echogenic tissue can be clearly observed. 10c. CT image of the thorax of a sheep with ovine respiratory complex. It can be seen a clear definition of ventral injured areas. White colour represents fluids inside alveoli, although bronchia maintain relatively empty their lumen.

Figure 11. 11a. Thorax radiography of a ewe with ovine pulmonary adenocarcinoma. Nodular pattern with different-sized nodules is observed. 11b. Thorax ultrasonography of a ewe with ovine pulmonary adenocarcinoma. Echogenic nodules with different sizes and shapes are shown. 11c. CT axial view of the thorax of a ewe with ovine pulmonary adenocarcinoma (soft tissue filter). Ventral lobes with consolidated areas and metastatic nodules in the rest of the lung are shown.

Figure 12. 12a. CT sagittal view of the thorax of a ewe with two verminous pneumonic areas in the dorsal left lung (white arrows). 12b. CT 3D sagittal view of the lung of a ewe with verminous pneumonia (volume rendering). Four foci are indicated in the dorsal lobe (white arrows).

Figure 13. 13a. CT sagittal view of the thorax of a ewe with caseous lymphadenitis in the

mediastinal lymph node (soft tissue filter) (white arrow). 13b. CT 3D image of caseous lymphadenitis affecting mediastinal lymph node (volume rendering) (white arrow). 13c. CT 3D image of caseous lymphadenitis (volume rendering) affecting mediastinal lymph node (white arrow).

Figure 14. 14a. Ultrasound image of the lung of a sheep affected of gangrenous pneumonia. Different echogenicity foci can be observed. 14b. CT sagittal view of the thorax of a ewe with gangrenous pneumonia (soft tissue filter). White arrow indicates the more severe affected areas with necrotic tissue within them. 14c. CT axial view of a gangrenous pneumonia in sheep (soft tissue filter) that show a huge necrotic area in the right lung (white arrow).

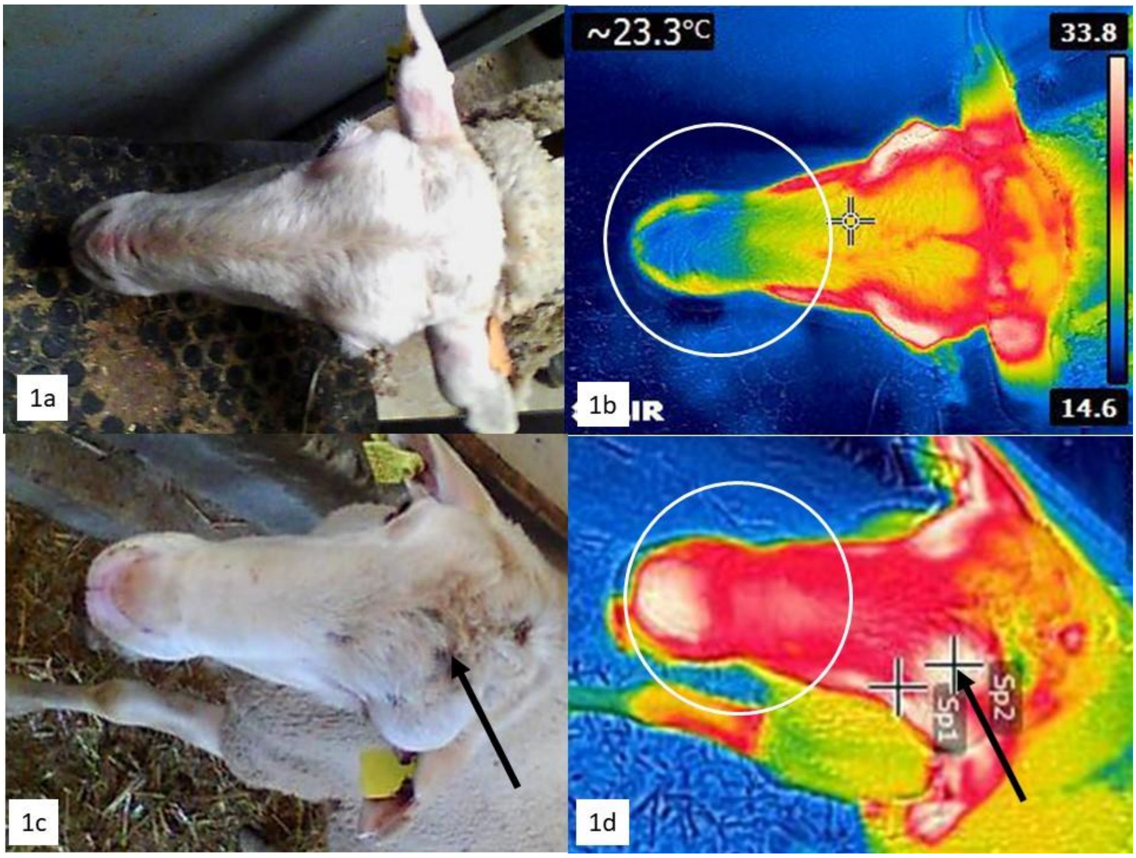

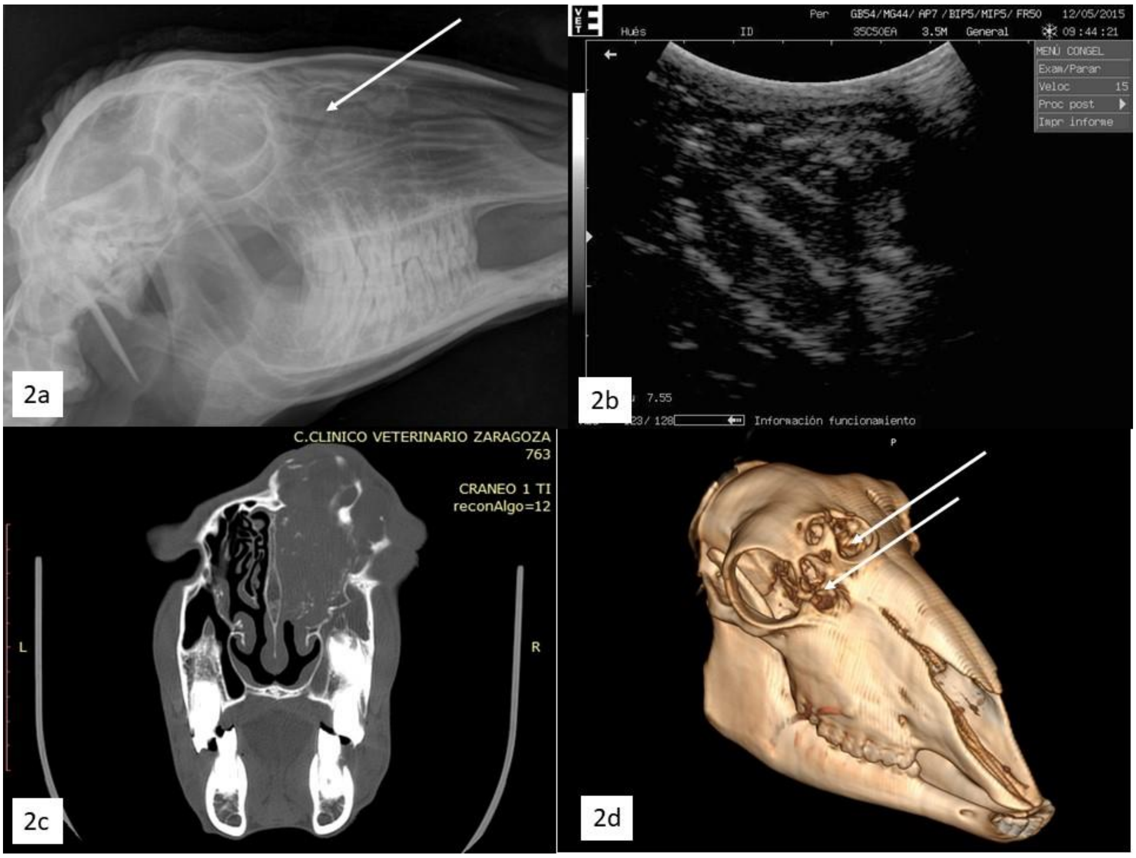
2a
Per GB54/MG44/ AP7 / BIP5/MIP5/ FR50 12/05/2015
Hués ID 35C50EA 3.5M General 09:44:21
MENÚ CONGEL
Exam/Parar
Veloc 15
Proc post
Impr informe
Información funcionamiento
2b
C.CLINICO VETERINARIO ZARAGOZA
763
CRANEO 1 TI
reconAlgo=12
L
R
2c
P
2d

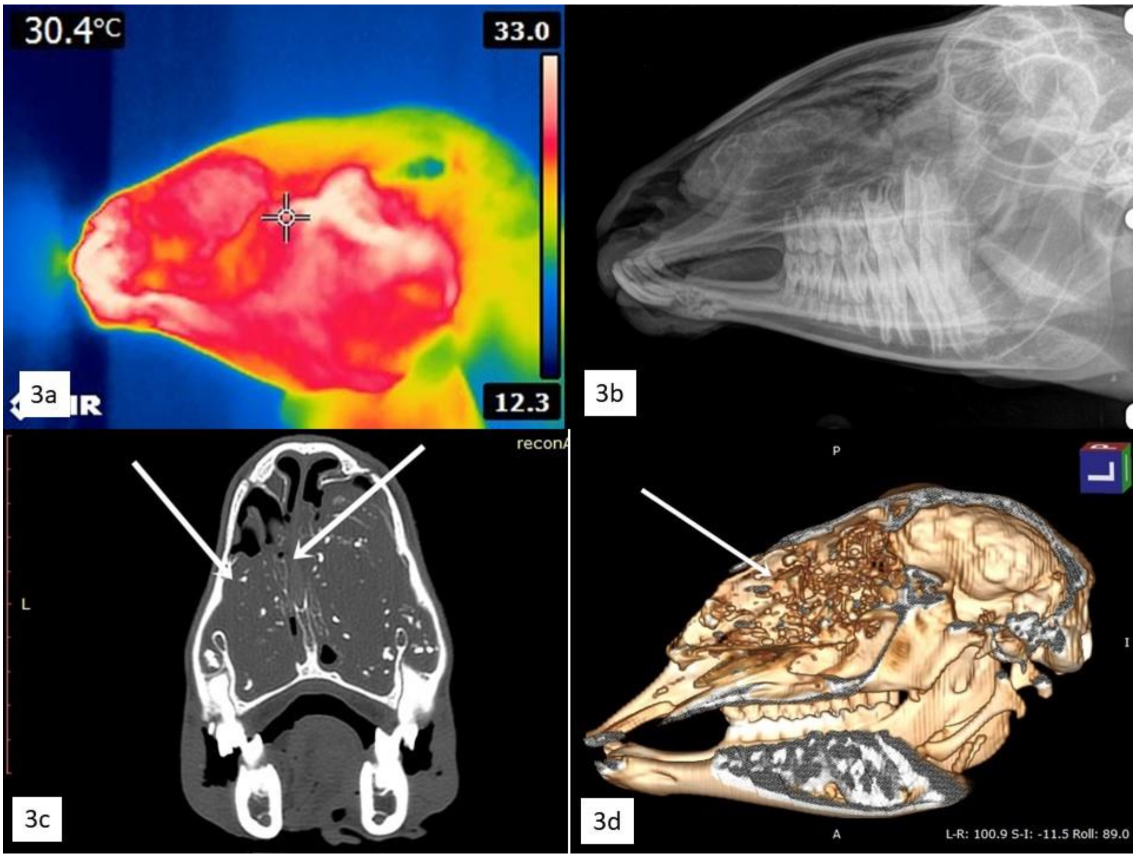
30.4°C
33.0
12.3
3a
3b
reconA
L
3c
P
A
I
L-R: 100.9 S-I: -11.5 Roll: 89.0
3d

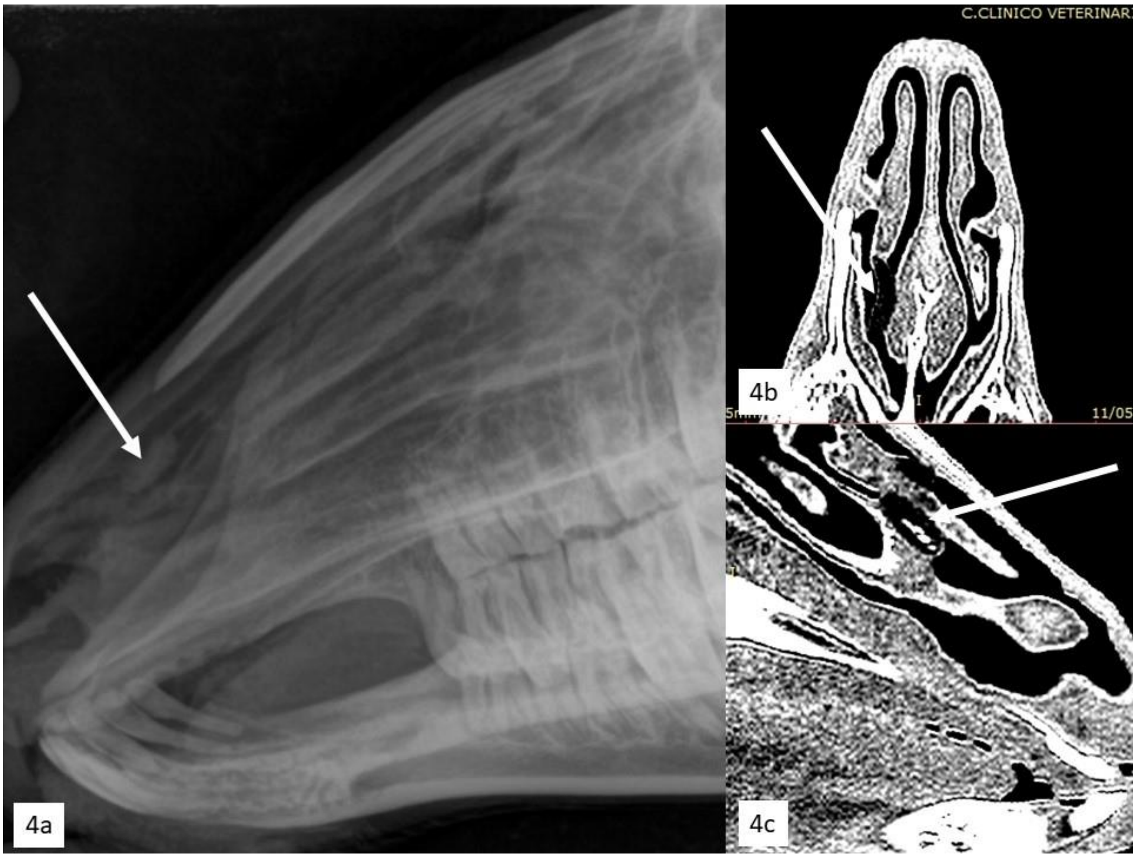
C.CLINICO VETERINARI
4a
4b
11/05
4c

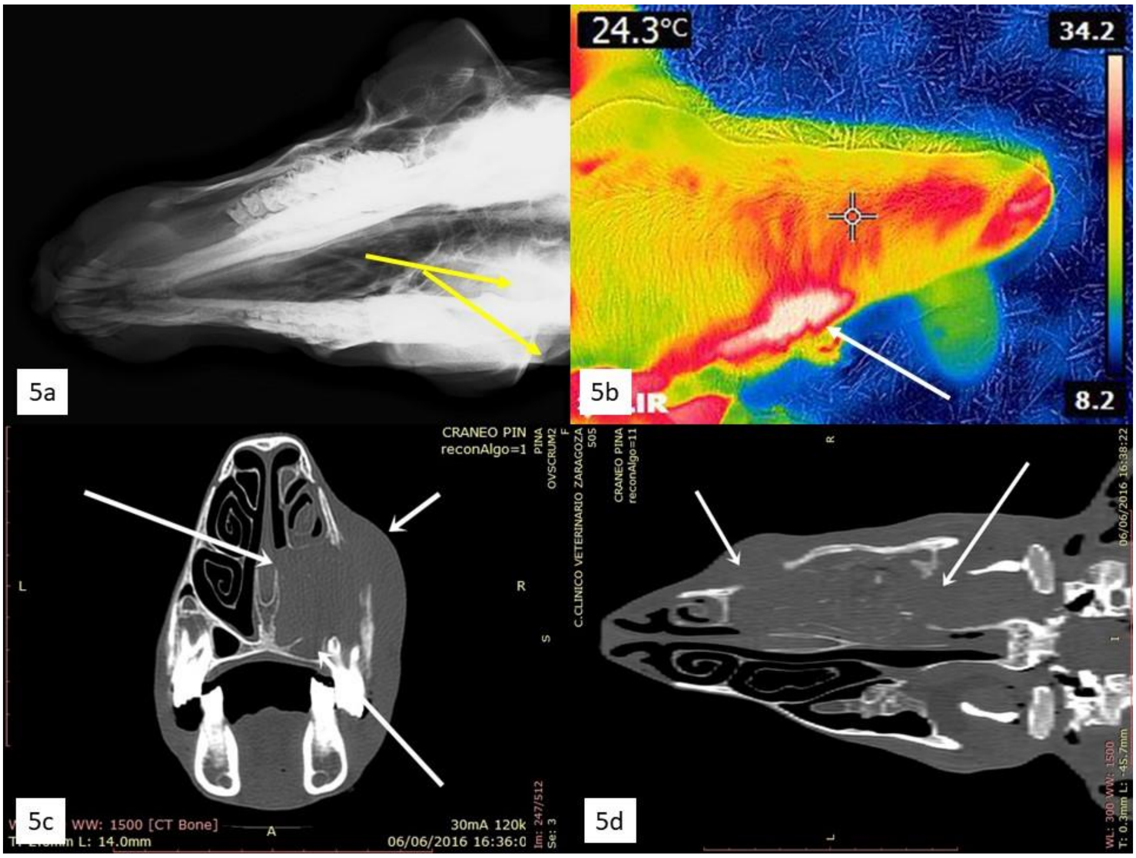
5a
24.3°C
34.2
8.2
5b
CRANEO PIN
reconAlgo=1
L
R
A
WW: 1500 [CT Bone]
L: 14.0mm
30mA 120k
06/06/2016 16:36:0
5c
C.CLINICO VETERINARIO ZARAGOZA
CRANEO PINA
reconAlgo=11
06/06/2016 16:38:22
5d

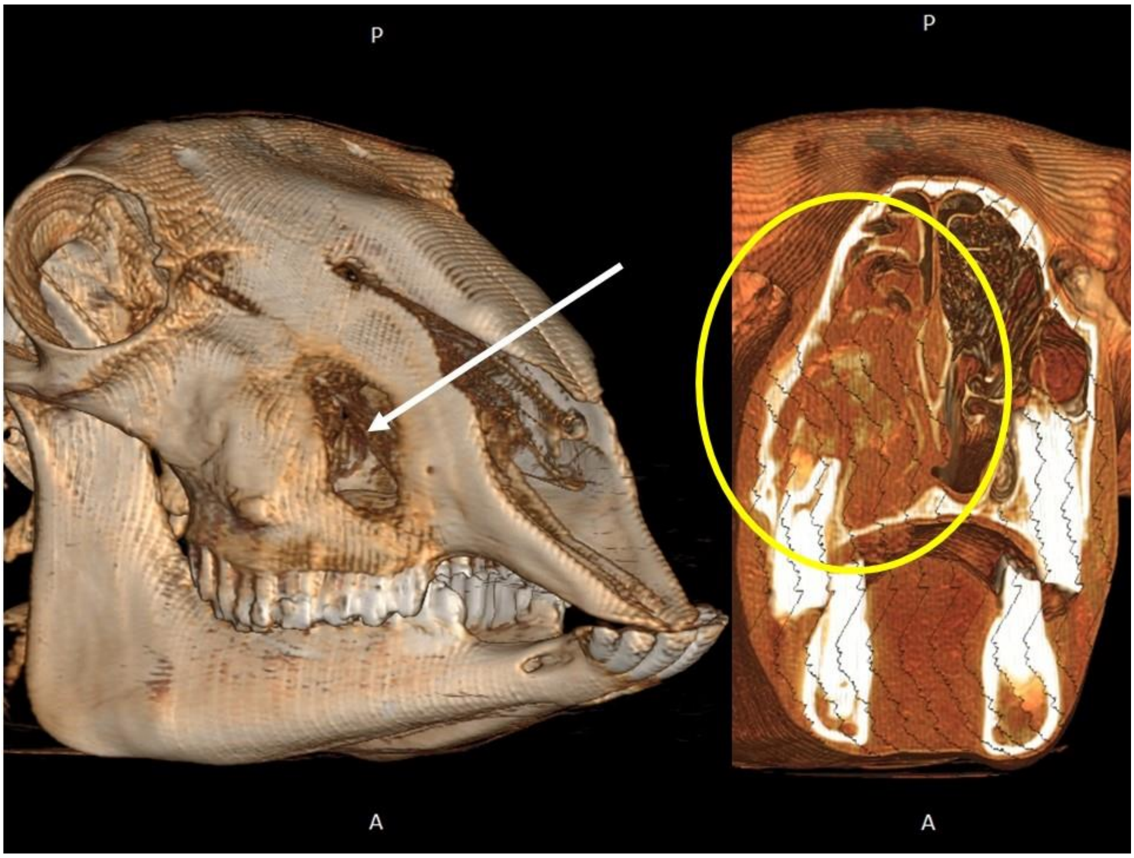
P
P
A
A

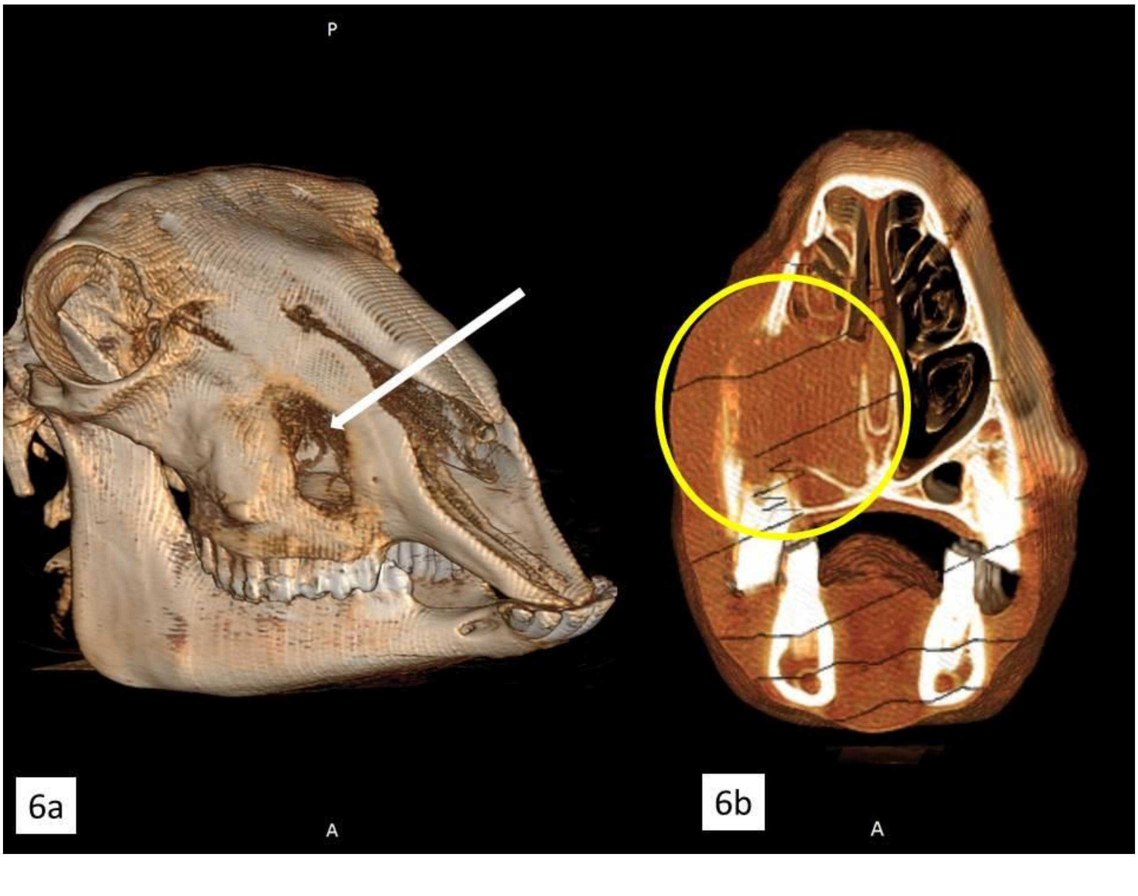
P
6a
A
6b
A

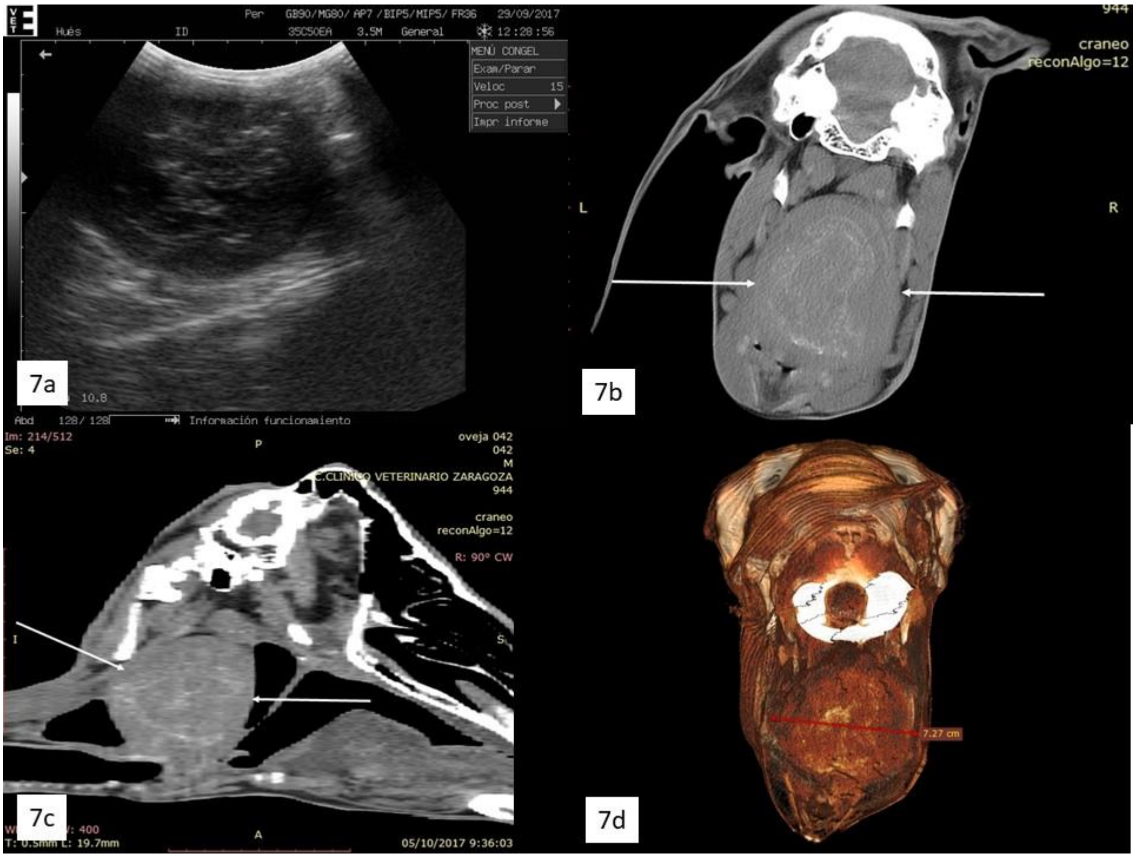
Per GB90/MG80/AP7/BIP5/MIP5/FR36 29/09/2017
Hués ID 35C50EA 3.5M General 12:28:56
MENÚ CONGEL
Exam/Param
Veloc 15
Proc post
Impr informe
7a
Abd 128/128 Información funcionamiento
944
craneo
reconAlgo=12
L
R
7b
Im: 214/512
Se: 4
P
oveja 042
042
M
C.CLINICO VETERINARIO ZARAGOZA
944
craneo
reconAlgo=12
R: 90° CW
I
S
7c
A
T: 0.5mm L: 19.7mm
05/10/2017 9:36:03
7.27 cm
7d

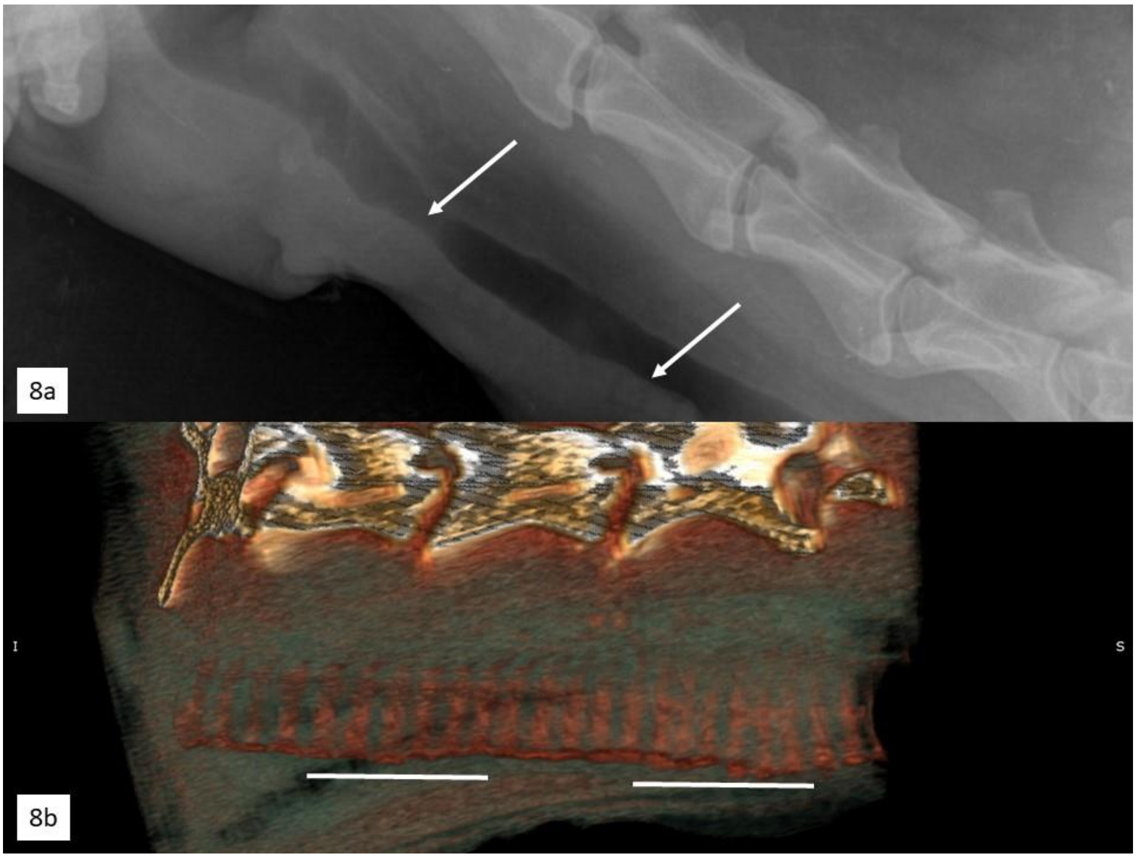
8a
I
S
8b

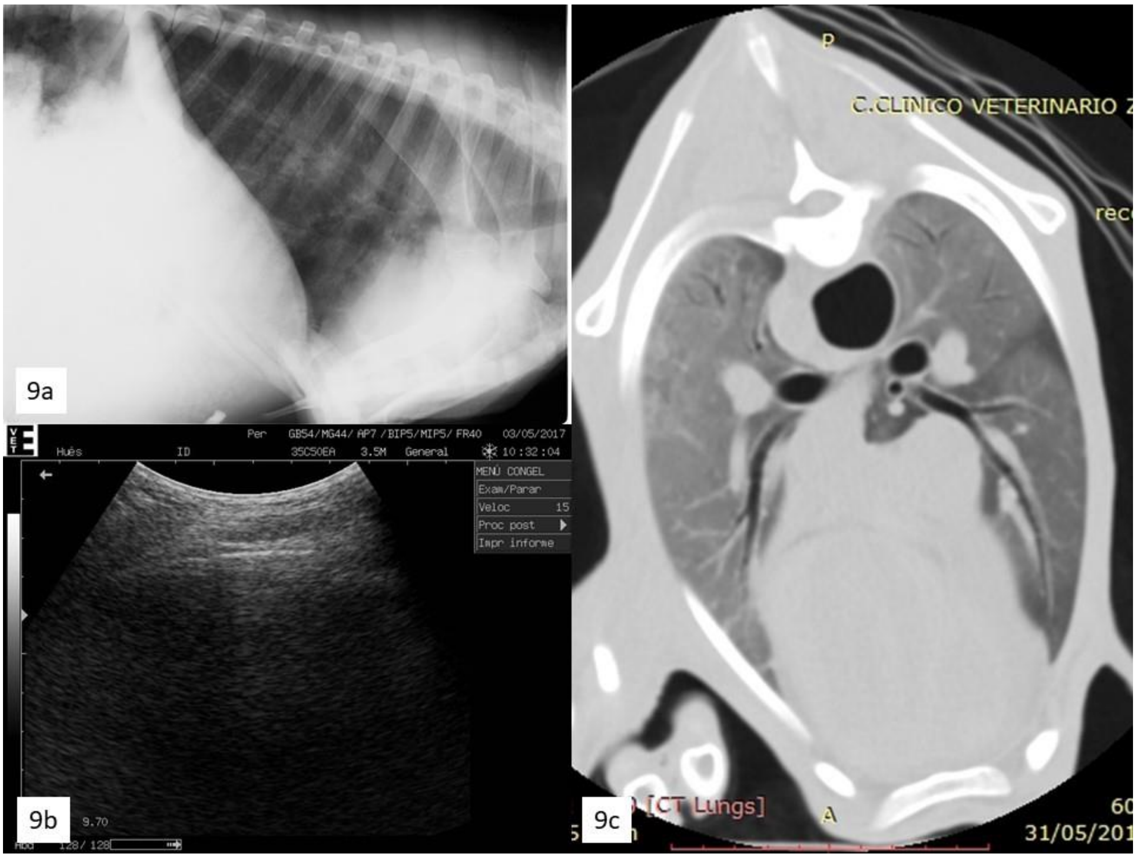
9a
9b
9c
C.CLINICO VETERINARIO
[CT Lungs]
31/05/201
P
A

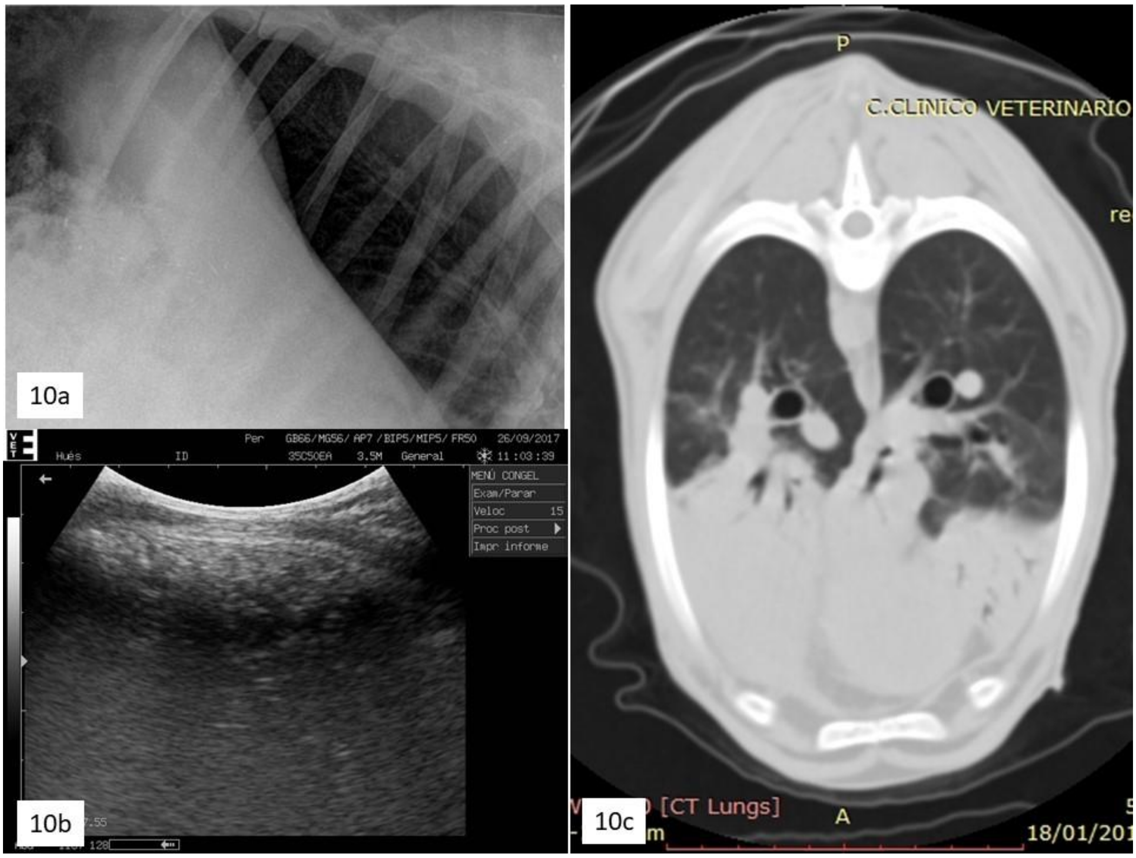
10a
10b
10c
C.CLINICO VETERINARIO
[CT Lungs]
18/01/201
P
A

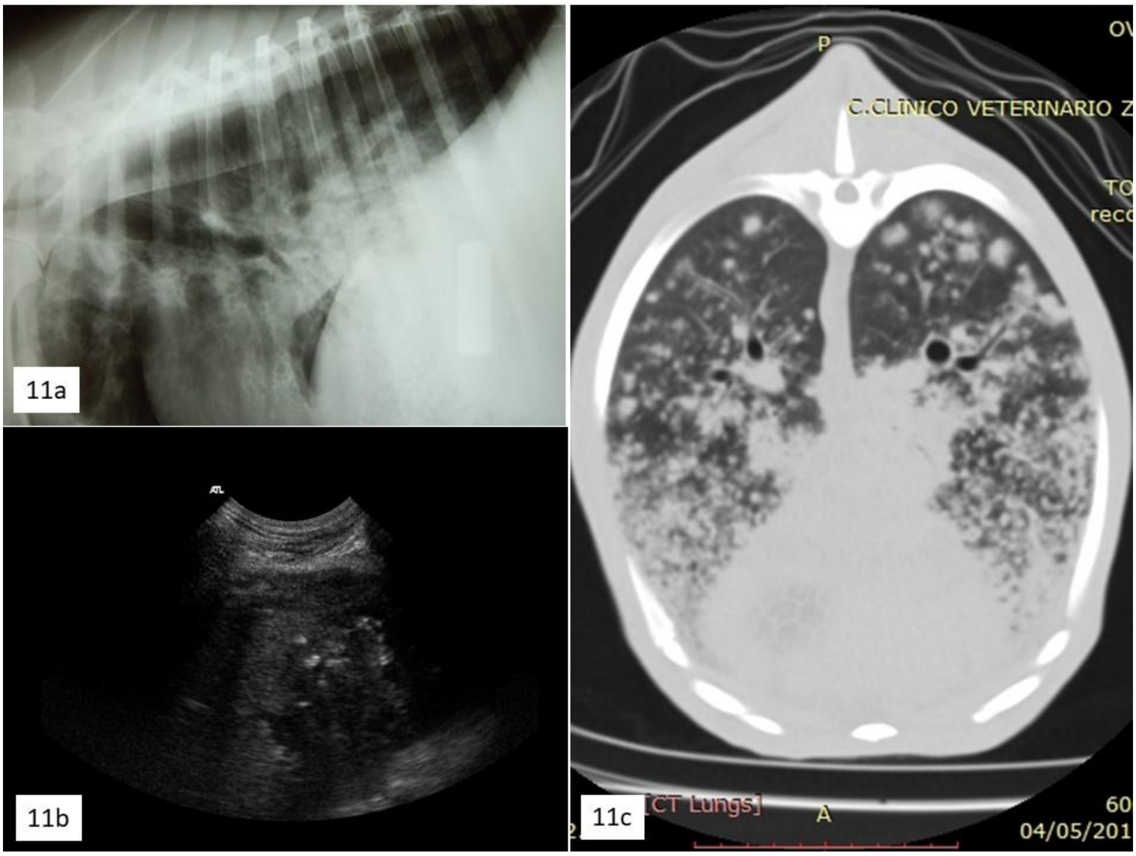
11a
11b
11c
ATL
P
A
[CT Lungs]

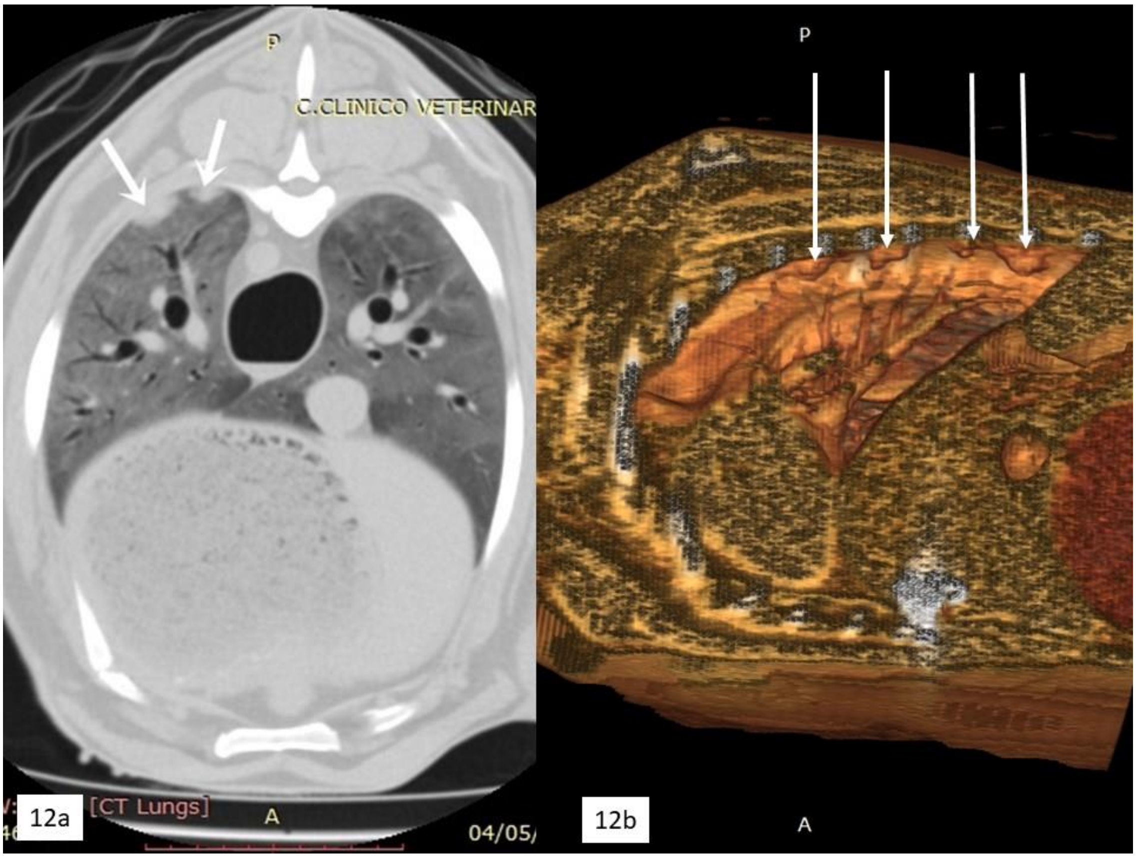
12a
12b
P
A
[CT Lungs]

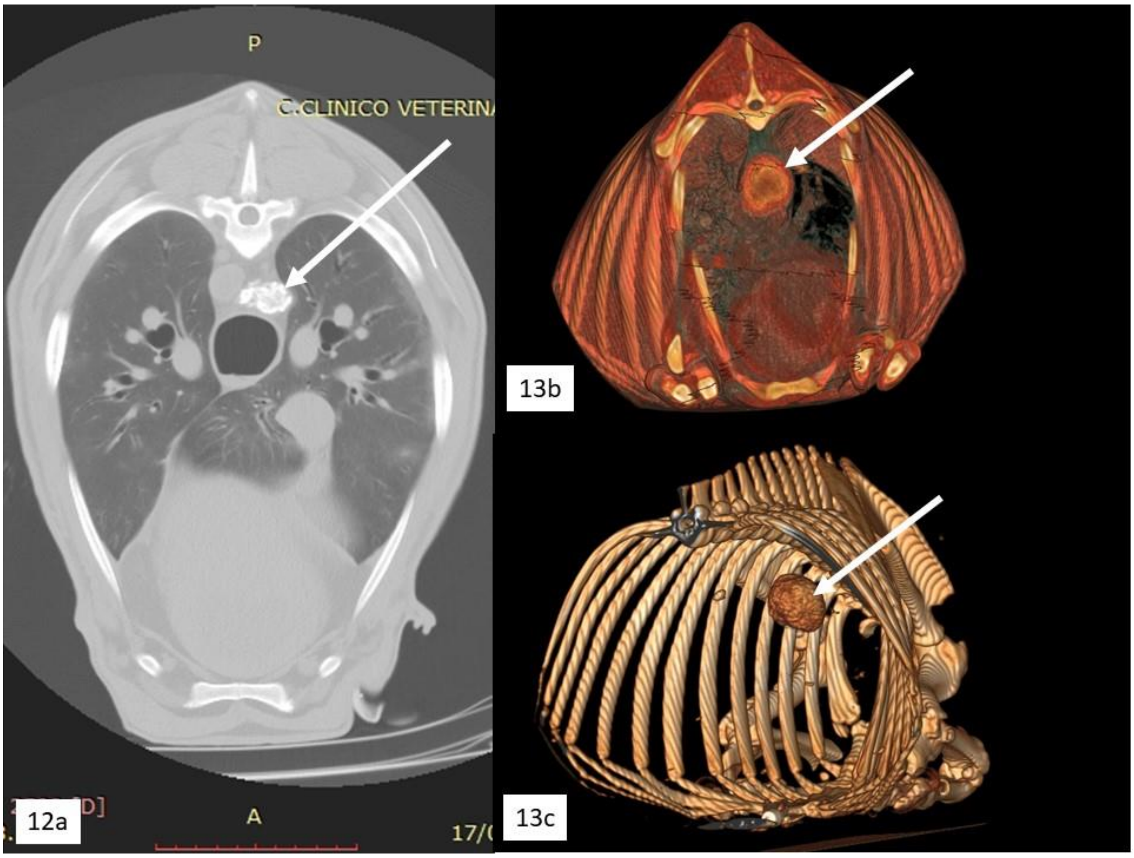
P
C.CLINICO VETERINA
A
12a
13b
13c

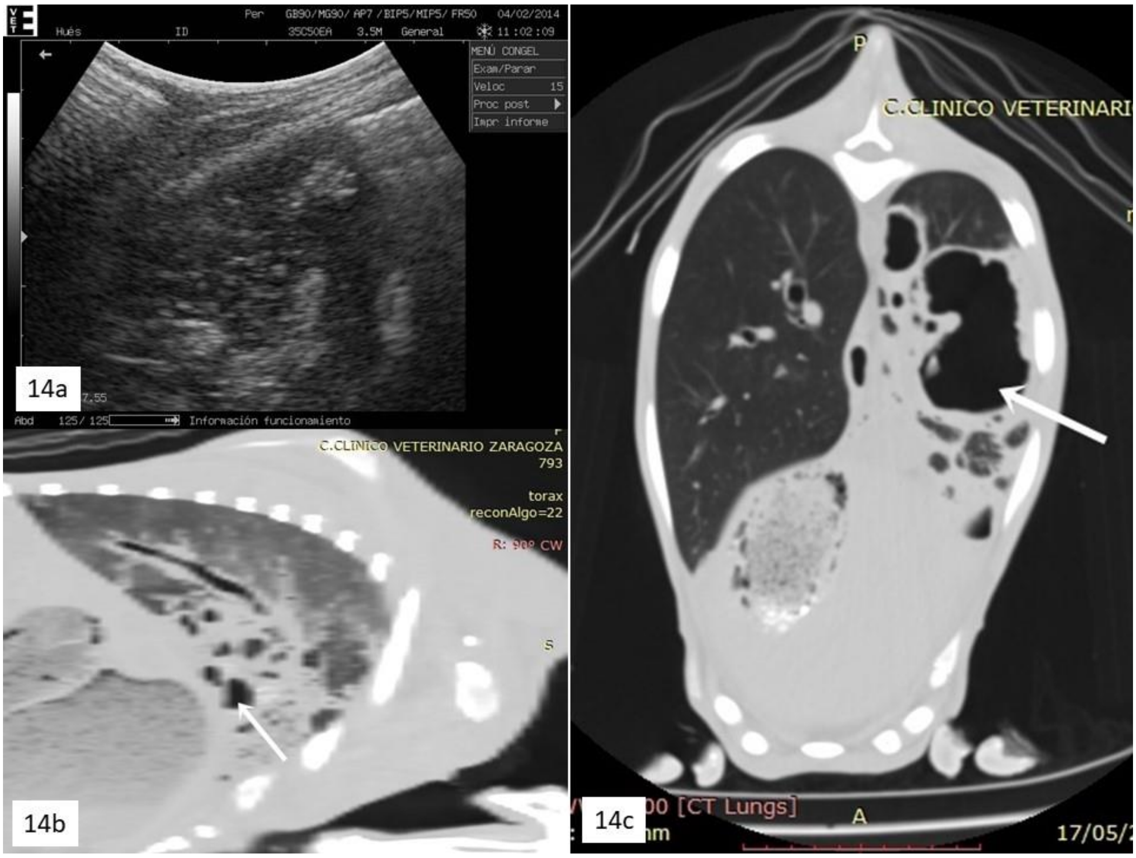
Per GB90/MG90/ AP7 / BIP5/MIP5/ FR50 04/02/2014
Hués ID 35C50EA 3.5M General 11:02:09
MENÚ CONGEL
Exam/Param
Veloc 15
Proc post
Impr informe
14a
Abd 125/ 125 Información funcionamiento
C.CLINICO VETERINARIO ZARAGOZA
793
torax
reconAlgo=22
R: 90º CW
S
14b
P
C.CLINICO VETERINARIO
[CT Lungs]
A
14c
17/05/